Bull Earthquake Eng (2011) 9:825–840
DOI 10.1007/s10518-011-9257-3

ORIGINAL RESEARCH PAPER

Peculiar earthquake damage on a reinforced concrete building in San Gregorio (L'Aquila, Italy): site effects or building defects?

Marco Mucciarelli · Marcello Bianca · Rocco Ditommaso · Marco Vona · Maria Rosaria Gallipoli · Alessandro Giocoli · Sabatino Piscitelli · Enzo Rizzo · Matteo Picozzi

Received: 9 December 2010 / Accepted: 26 February 2011 / Published online: 22 March 2011

Abstract In San Gregorio (L'Aquila, Italy) a three-story, reinforced concrete (RC) building had the first floor collapsed following the earthquake of April 6, 2009. The remaining two stories fell with a displacement in the horizontal projection of about 70 cm. This unusual behaviour is made more puzzling by the fact that buildings located at a short distance and with similar features had little or no damage reported. To understand the causes of the collapse we performed strong motion recordings, microtremor measurements, a detailed geological survey, a high-resolution geo-electrical tomography, a borehole with a down-hole test. On the building we performed a geometrical survey and laboratory tests on concrete cores. The acceleration and noise recordings have shown a high amplification with uphill-downhill direction. The geological survey has revealed the presence of co-seismic fractures on stiff soils. Geo-electrical tomography has shown an unexpected, strong discontinuity just below the building. Taking advantage of excavations in adjacent lots, we have highlighted rare cataclastic decimetric bands with a very low resistance material incorporated in well-stratified calcarenites. The same soft material has been founded in the borehole down to 17 m from ground level, showing a shear wave velocity that starts at 250 m/s, increases with depth and has an abrupt transition in calcarenites at 1,150 m/s. The surface geophysical measurements in the vicinity of the site have not shown similar situations, with flat HVSR curves as expected for a rock outcrop, except for a lateral extension of the soft zone. The analysis on the quality of the building materials has yielded values higher than average for the age and type of construction, and no special design or construction deficiencies have been observed. A strong, peculiar site effect thus appears to be the most likely cause of the damage observed.

M. Mucciarelli · M. Bianca · R. Ditommaso · M. Vona (✉)
Department of Structures, Geotechnics, Engineering Geology, University of Basilicata, Potenza, Italy
e-mail: marco.vona@unibas.it

M. R. Gallipoli · A. Giocoli · S. Piscitelli · E. Rizzo
IMAA-CNR, Tito Scalo, Potenza, Italy

M. Picozzi
Deutsches GeoForschungs Zentrum GFZ, Section 2.1, Helmholtzstraße 7, 14467 Potsdam, Germany

Keywords L'Aquila earthquake · Structural damage · RC building · Site effects · Strong motion recordings

1 Introduction

The 2009 L'Aquila earthquake caused a remarkably variable pattern of damage distribution at different scales. The macroseimic survey performed immediately after the mainshock (Galli and Camassi 2009) showed a clear sign of directivity SW of the epicentre, and a strong variation of intensity between towns few kilometres apart. The San Gregorio village is close to the macroseismic epicentre, about 15 km from the instrumental one. In a radius of less than 5 km, the intensity varies from the maximum (the only degree X MCS, assigned to the village of Onna) to the limit of damage (degree VI MCS). San Gregorio has intensity equal to IX MCS, but this is due to the combination of two different level of damage (Fig. 1).

As it can be seen in Fig. 2, the core of San Gregorio is a dense historical centre, with prevailing masonry building even centuries old. The entire area suffered heavy structural damage, with several collapses that caused 14 casualties. Eastward and westward of the historical centre, a less dense urbanization prevails, mainly with single-family houses with gardens. Most of the houses in this expansion area are RC buildings. The damage here is moderate, with few structural damages, no collapses and several undamaged buildings that remained inhabited along the whole seismic sequence. The only exception in this area is the three-storey RC building subject of our study, that suffered a collapse of the first floor while the two upper floors remained standing. It is worth noting that the damage of the historical centre was due not only to the higher vulnerability of buildings, but also to site seismic amplification: the area was built on an alluvial fan. On the contrary the expansion areas are

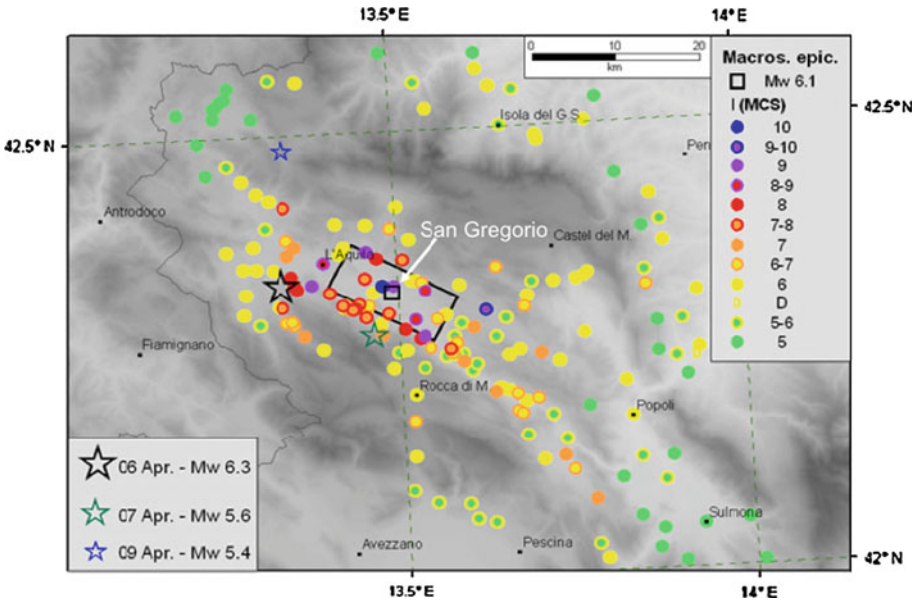

Fig. 1 Intensity map of the L'Aquila, 2009 earthquake (modified from QUEST 2009)

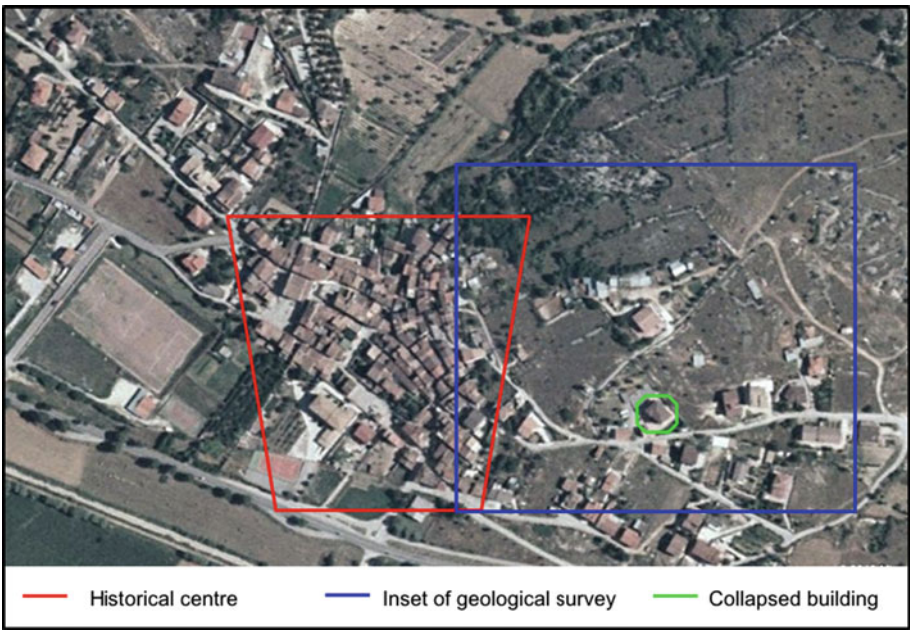

Fig. 2 Aerial view of the San Gregorio village prior to the 2009 earthquake

built on outcropping rock (see Compagnoni et al. 2010 for details on the microzonation study relevant to San Gregorio).

2 Building characteristics and observed damage

The project of the building and then the related age of the construction range from 1978 to 1980. As a consequence of the 1915 Avezzano earthquake, L'Aquila town and surrounding villages have been seismic classified since then. The building under study was designed taking into account the seismic Italian Code enforced at time of construction. According to that code, seismic actions were carried out considering the static equivalent horizontal forces applied to plane frames in the two orthogonal directions. Consequently, internal beams are spanning both in longitudinal and transversal direction. The building has a Reinforced Concrete (RC) framed structure with three storeys, tilted roof and the floors are RC slabs with thickness equal to 20 cm. The 3D framed structure is two by three bays (5 m long, width varies between 3.90 and 4.6 m) and inter-storey height is equal to 3.2 m. The foundation system is made by shallow foundations (T beams).

Compatibly with the building conditions, investigation on elements dimension and reinforcement details has been carried out in order to evaluate the global quality of the original design and construction of the building. In order to identify the structural system and its dimensions, as well as the collapse mechanism, a visual survey on the structure has been carried out. Moreover, dimensions and details of reinforcing steel have been detected and compared with those obtained by the original design (Fig. 3).

The building can be considered as having approximately regular shape in elevation. Column sizes are variable at each storey. At the ground storey, the columns have 30×50 cm

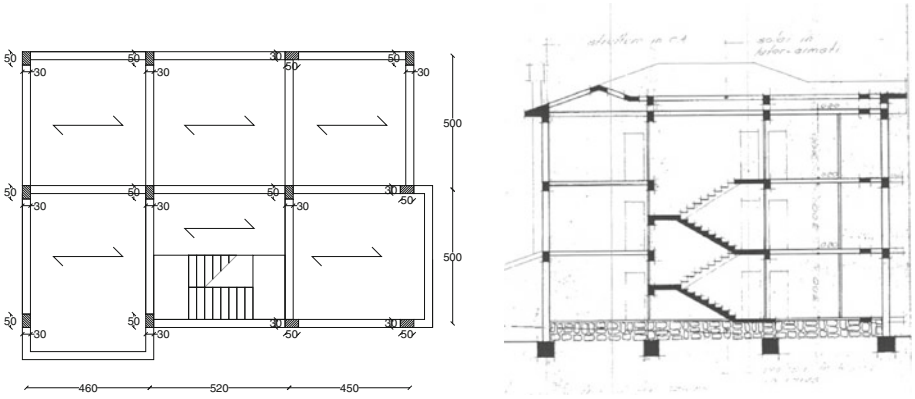

Fig. 3 In plan (units are cm) and transversal sections of the studied building

dimensions, decreasing to 30 × 45 and 30 × 40 cm at the first and second storey, respectively. For internal beams the transversal section is equal to 30 × 50 cm and in some cases 50 × 20 cm. The staircase is made up of beams with section supporting the stair-tilted slabs. Infills are made of two layers of hollow brick masonry. With regard to seismic design, it is necessary to consider that the studied building had a seismic design and structural details (Fig. 4a, b) that did not appear different to those of similar RC buildings located in L'Aquila town and in neighbouring villages. Moreover, this building appears to have a good quality of construction if compared with others built in the surrounding area. Unfortunately, as discussed in other works (Mucciarelli et al. 2004; 2011; Masi and Vona 2010) the structural details, even if consistent with the requirements of the code enforced at time of construction, showed that this building is not very different from RC buildings designed to resist to vertical loads only. At this point, the structural details have been surveyed and some tests on material characteristics have been carried out.

As mentioned above, some cores have been tested in laboratory to evaluate their cylinder compression strength $f_{c,core}$. These core test values have been converted into the equivalent in situ values by mean the following expression (Dolce et al. 2006):

$$f_c = \left(C_{H/D} \cdot C_{dta} \cdot C_a \cdot C_d\right) \cdot f_{c,core}$$

where:

$C_{H/D}$ = correction for height/diameter ratio H/D, equal to $C_{H/D} = 2/(1.5 + \mathrm{D/H})$;
C_{dta} = correction for diameter of core D, equal to 1.06, 1.00 and 0.98 for D, respectively equal to 50, 100 and 150 mm;
C_a = correction for the presence of reinforcing bars, equal to 1 for no bars, and varying between 1.03 for small diameter bars (Φ 10) and 1.13 for large diameter bars (Φ 20);
C_d = correction for damage due to drilling.

Finally, the average value of the in situ concrete strength was been obtained: $f_{cm} = 28.1$ MPa. This value has been compared with experimental results of in situ concrete strength obtained by existing RC buildings (Masi and Vona 2009). The experimental results show that in situ concrete strength is remarkably dependent on the period of construction (Fig. 5). Average values of f_c are in good agreement with the expected values relevant to the standards of the time of the construction $f_{cm,def}$. Moreover, it is worth noting that the above experimental strength evaluated for the San Gregorio RC building is higher than the

Fig. 4 Storey mechanism: details of the columns on back view (**a**); structural column details (**b**); lateral view (East) (**c**); back view (North) (**d**)

average value of the construction period (Fig. 5c). Finally, considering the global quality of the building, it is possible to exclude detrimental conditions or deterioration of materials.

With regard to the damage mechanism of the studied building, it was possible to observe a storey mechanism. In Fig. 4c, d some significant images of the collapse are reported. It can be seen that only the first floor has been affected by the structural damage, but probably this fact does not implies a significant difference of stiffness with the other floors (all the floors had infills and the height was equal). The collapse was due to a significant shift (estimated at about 40 cm) on the first floor. As consequence, the columns of the first floor were cut at the top section (close to the beams). This mechanism may have been facilitated by both the poor anchoring of the bars and the fact that the beam-column joint that was not cast monolithically.

3 Geologic survey and borehole

In order to map out the geological and structural features of the area of San Gregorio where the collapsed building stood, a detailed geologic survey has been carried out, starting from the two geological maps already available for this area, namely the 'Sheet 349 L'Aquila' of the

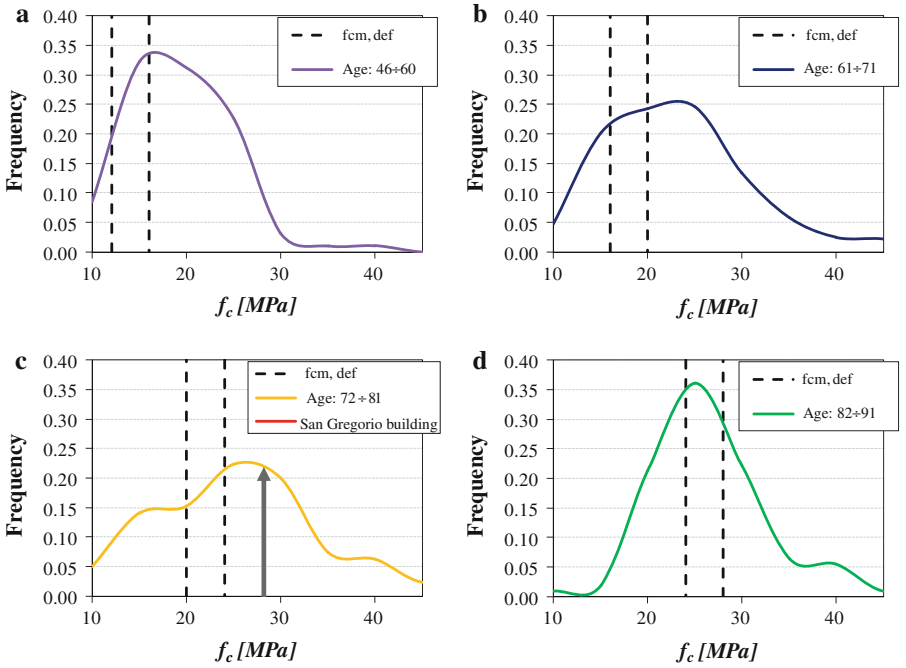

Fig. 5 Distribution of in situ strength values f_c vs $f_{cm,def}$ (mean default values in various construction periods). In panel **c** the experimental value for the San Gregorio RC building is reported as a straight line

CARG Project (scale 1:50,000) and the 'Geological map of the Paganica-S.Gregorio area' (scale 1:5,000), the latter drawn after the earthquake in the framework of the microzonation project launched by the Department of Civil Defence (Compagnoni et al. 2010). The results of the geological survey are shown in Fig. 6.

The collapsed building is located on a slightly-dipping ridge characterized by the outcropping of a well-stratified succession of calcarenites which belongs to the 'Scaglia Cinerea' formation of the 'Monte Pettino' unit in the geological Sheet 349. The mean attitude of the calcarenitic strata is generally S-dipping with dip angles ranging from 7° to 30°. The lower part of the slope is covered by the Upper Pleistocene-Holocene alluvial deposits of the Aterno valley and by the alluvial-fan deposits coming from a small lateral valley.

The main structural features in this area are represented by two normal faults, whose surface traces are covered by the Upper Pleistocene-Holocene alluvial deposits (Fig. 6). In particular, the NW-SE trending normal fault (SW edge of the map in Fig. 6) is considered as still active.

In Fig. 6, the alignment of the co-seismic ground fractures detected and mapped in the first days after the mainshock is also reported, which shows the same NW-SE trend of the active normal fault.

On the contrary, several decimetric cataclastic bands that cross-cut the Miocene calcarenites (Fig. 7) are characterized by a NE-SW direction that mimics the trend of the other normal fault.

Few meters west from the collapsed building, a 22 m deep geognostic borehole has been drilled, and inside it a down-hole test has been performed. The stratigraphy of the borehole and the results of the down-hole test are shown in Fig. 8. At the borehole point, the stratigraphical

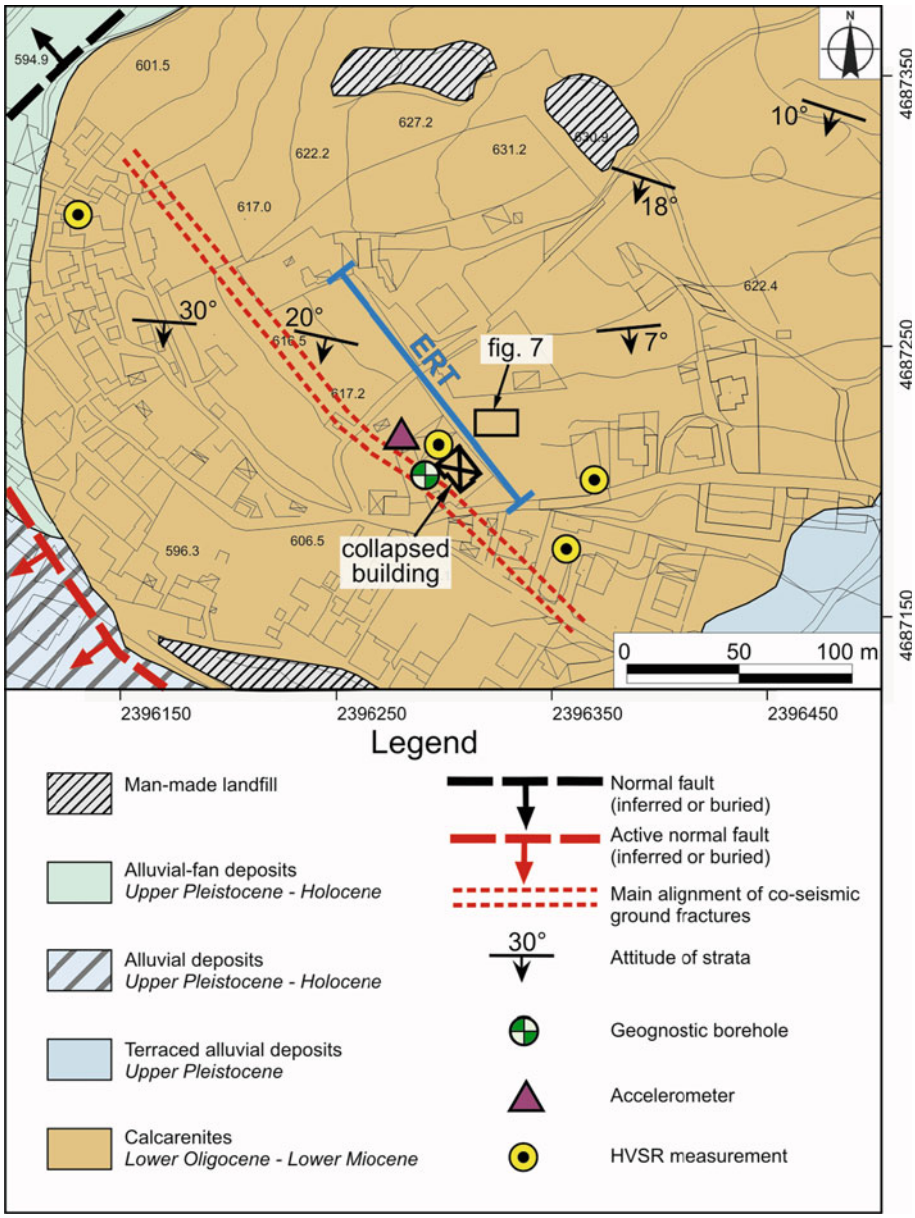

Fig. 6 Geological map of the area where the collapsed building stood. The locations of the geophysical tests and the geognostic borehole are also reported

succession is made up of about 15 m of scarcely cemented breccias with sandy matrix, overlying the Miocene calcarenites which show a moderate degree of fracturation. The velocities of the shear waves obtained through the down-hole test gradually increase with depth across the breccias, with an abrupt step from about 200 m/s to about 1,000 m/s between the depth of 4–12 m.

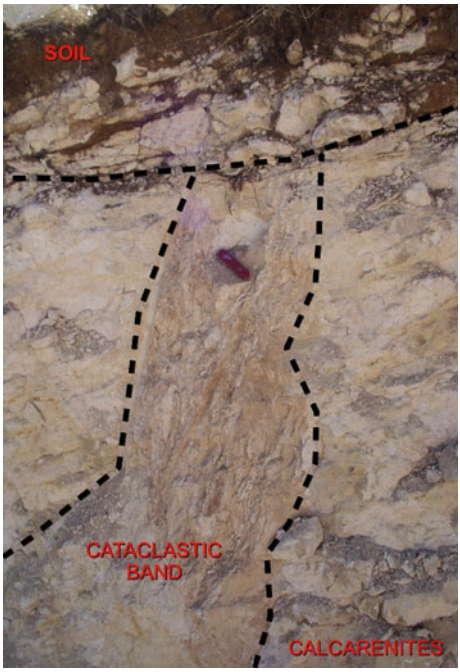

Fig. 7 Photograph of the outcropping calcarenites with decimetric cataclastic band. See Fig. 6 for location

4 Geo-electrical survey

To understand the causes of the collapse, the subsurface of the investigated area has been investigated also by means of a 2D Electrical Resistivity Tomography (ERT), which has been compared and calibrated with geological survey, other geophysical measurements and borehole data. The trace of the profile along which the ERT was carried out is reported in Fig. 6.

The electrical imaging or ERT is a geo-electrical method, widely applied to obtain 2D and 3D high-resolution images of the resistivity subsurface patterns in areas of complex geology (Griffiths and Barker 1993; Sharma 1997; Giano et al. 2000; Dahlin 2001; Caputo et al. 2003; Galli et al. 2006). Technically, an ERT survey can be carried out using different electrode configurations that are dislocated on earth surface to send into the ground the electric currents and to measure the generated voltage signals (for details about field procedure see Caputo et al. 2003 and references therein).

Resistivity field data were collected with a Syscal R2 earth resistivity meter of Iris Instruments coupled to a multielectrode system. A Wenner-Schlumberger array with 28 electrodes, 5 m spaced, was used, obtaining an electrical image 135 m long and with an investigation depth of about 25 m. The Res2dinv resistivity inversion software (Loke 2001) was used to automatically invert the apparent resistivity data from the field. The inversion routine is based on the smoothness constrained least-squares inversion (Sasaki 1992) implemented by using a quasi-Newton optimization technique. The subsurface is divided into rectangular blocks, the number of which corresponds to the number of measurement points. The optimization method adjusts the 2D resistivity model trying to iteratively reduce the difference between

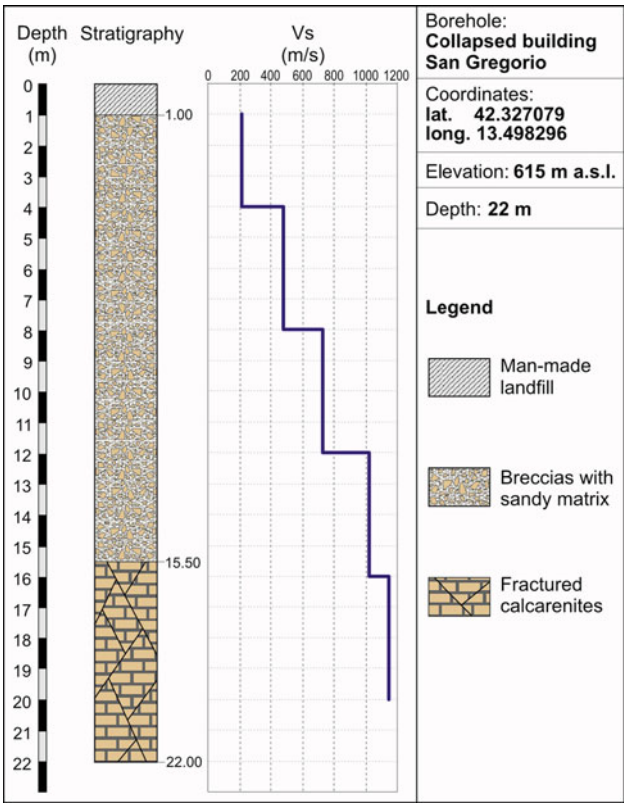

Fig. 8 Geognostic borehole performed in the foundation soil of the collapsed building. See Fig. 6 for location

the calculated and measured apparent resistivity values. The root-mean-squared (RMS) error provides a measurement of this difference (Loke 2001).

Figure 9 shows the inverted electrical resistivity model for the section along the collapsed building. To achieve the best fit, four iterations were performed, obtaining a RMS error equal to 3.8%. The resistivity values range from 70 to over 1, 778 Ωm.

The electrical image shows, in the whole, a resistivity pattern characterized by three electrical layers, the central one relatively conductive. The most outstanding feature is certainly the relatively low resistivity zone ($\rho < 200\,\Omega$m) just below the collapsed building.

On the basis of both geological and borehole data, this configuration could be due to different physical (electrical) properties of the same lithotype (calcarenite), rather than to the presence of different lithological horizons. In particular, the deep high resistivity zone ($\rho > 650\,\Omega$m) could be associated with massive calcarenitic bedrock (CFR2), as found in the borehole at a depth of about 15–16 m from ground level. The relatively conductive central layer, which presents resistivity values down to 70 Ωm in the left-hand zone, and the thin resistive surface layer could be associated with the same calcarenitic bedrock, but intensely fractured and with the likely presence (CFR2-FH) or absence (CFR2-F) of water. Furthermore, in the central part of the electrical image, the occurrence of a strong step in the lateral resistivity distribution could to be due to the presence of a fault plane.

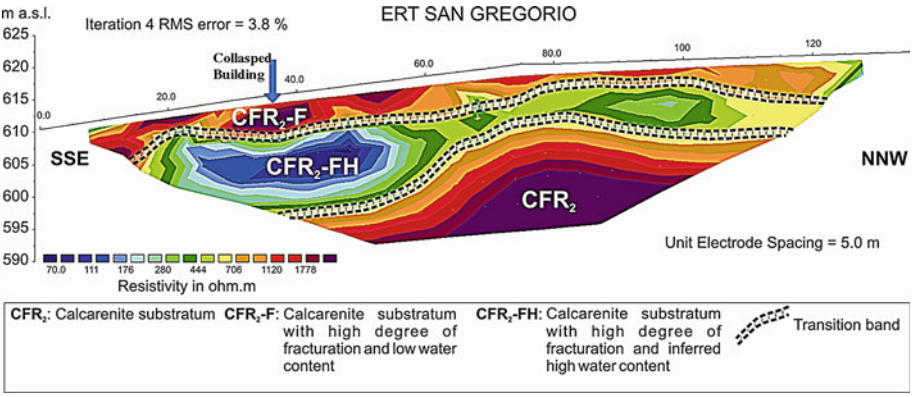

Fig. 9 Electric resistivity tomography carried out on a section passing close to the collapsed building located at about 40 m from origin. See Fig. 6 for location details

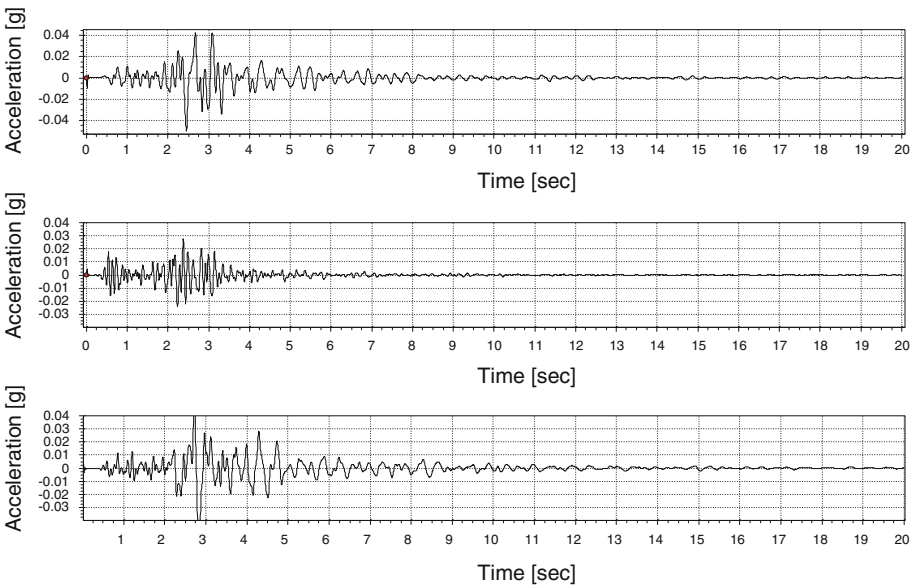

Fig. 10 Acceleration recordings of the $M_l = 4.0$ shock on April, 23rd at 15.14. Components are NS (*upper*), UD (*middle*) and EW (*lower*)

5 Strong motion and ambient noise recording

To understand if seismic site amplification could be a possible cause of damage we have performed several ambient noise and earthquake recordings. The aftershocks were recorded by the accelerometer Kinemetrics Altus K2 installed by German Task Force (GFZ-Potsdam) close to the collapsed building two days after the mainshock and uninstalled on April 26. Figure 6 reports the location of the station. The magnitude of the recorded earthquakes ranges between 3.0 and 4.0 Ml and the epicentral distance between 10 and 40 km. Table 1 reports the principal characteristics of these seismic events, while Fig. 10 reports the acceleration recordings of the strongest aftershock recorded, $M = 4.0$ on April 23rd at 15:14.

Table 1 Principal characteristics of the seismic events recorded near the collapsed building

Data and UTC hour	Magnitude (MI)	Lat.	Lon.	Depth	Epicentral area
10/04/2009 19:07	3.1	42.38	13.39	9.5	Aquilano
10/04/2009 19:18	3	42.34	13.36	10.2	Aquilano
11/04/2009 05:39	3.3	42.39	13.4	10.7	Aquilano
11/04/2009 06:13	3	42.47	13.42	9.1	Gran Sasso
11/04/2009 06:57	3.2	42.39	13.41	10.5	Aquilano
11/04/2009 07:04	3.2	42.39	13.41	11	Aquilano
11/04/2009 15:42	3.1	42.52	13.32	8.7	Monti della Laga
11/04/2009 19:53	3	42.35	13.53	9.8	Valle dell'Aterno
12/04/2009 03:29	3.1	42.54	13.32	9.7	Monti della Laga
12/04/2009 09:48	3.2	42.36	13.38	10.1	Aquilano
12/04/2009 16:35	3.2	42.52	13.38	10.1	Monti della Laga
12/04/2009 18:05	3.4	42.4	13.39	9.8	Aquilano
12/04/2009 18:09	3	42.29	13.5	10.4	Valle dell'Aterno
18/04/2009 11:07	3.2	42.27	13.49	9.4	Valle dell'Aterno
18/04/2009 13:03	3.1	42.33	13.5	10.2	Valle dell'Aterno
20/04/2009 02:22	3	42.38	13.32	10.5	Aquilano
23/04/2009 15:14	4	42.25	13.49	9.9	Velino-Sirente
23/04/2009 21:49	4	42.23	13.48	9.3	Velino-Sirente
24/04/2009 04:36	3	42.26	13.47	10.3	Velino-Sirente
24/04/2009 13:38	3.2	42.52	13.35	9.4	Monti della Laga
24/04/2009 14:24	3	42.39	13.39	8.3	Aquilano
24/04/2009 15:53	3	42.31	13.47	10.5	Aquilano
24/04/2009 22:51	3	42.27	13.51	11	Valle dell'Aterno
25/04/2009 02:08	3.1	42.29	13.45	8.3	Aquilano
25/04/2009 11:13	3	42.42	13.33	9.1	Aquilano
25/04/2009 13:17	3	42.26	13.5	10.9	Valle dellAterno
26/04/2009 17:56	3.3	42.46	13.38	10.6	Gran Sasso

The ambient noise recordings, 20–30 min long, have been acquired by a digital tri-directional tromometer (Micromed Tromino), which is a high-resolution seismometer whose 24-bit dynamic is aimed at the very low amplitude range. The Horizontal-to-Vertical Spectral Ratio (HVSR) curves for ambient noise were calculated by averaging the HVSR obtained by dividing the signal into non-overlapping windows of 20 s. Each window was detrended, tapered, padded, FF-Transformed and smoothed with triangular windows with a width equal 5% of the central frequency. The average was used to combine EW and NS components in the single horizontal (H) spectrum. Average single component spectra were obtained from the same procedure. For each HVSR curve the relative $\pm 2\sigma$ confidence interval is given. We did not perform any window selection, using the whole traces for both the noise recording and the earthquakes (Parolai and Galiana-Merino 2006; Chatelain et al. 2008).

We have performed several ambient noise recordings (see Fig. 6 for location). Far from the collapsed building the HVSR curves are flat as expected on outcropping well-cemented Miocene calcarenites. On the contrary, the HVSR curve close to the building (Fig. 11) shows

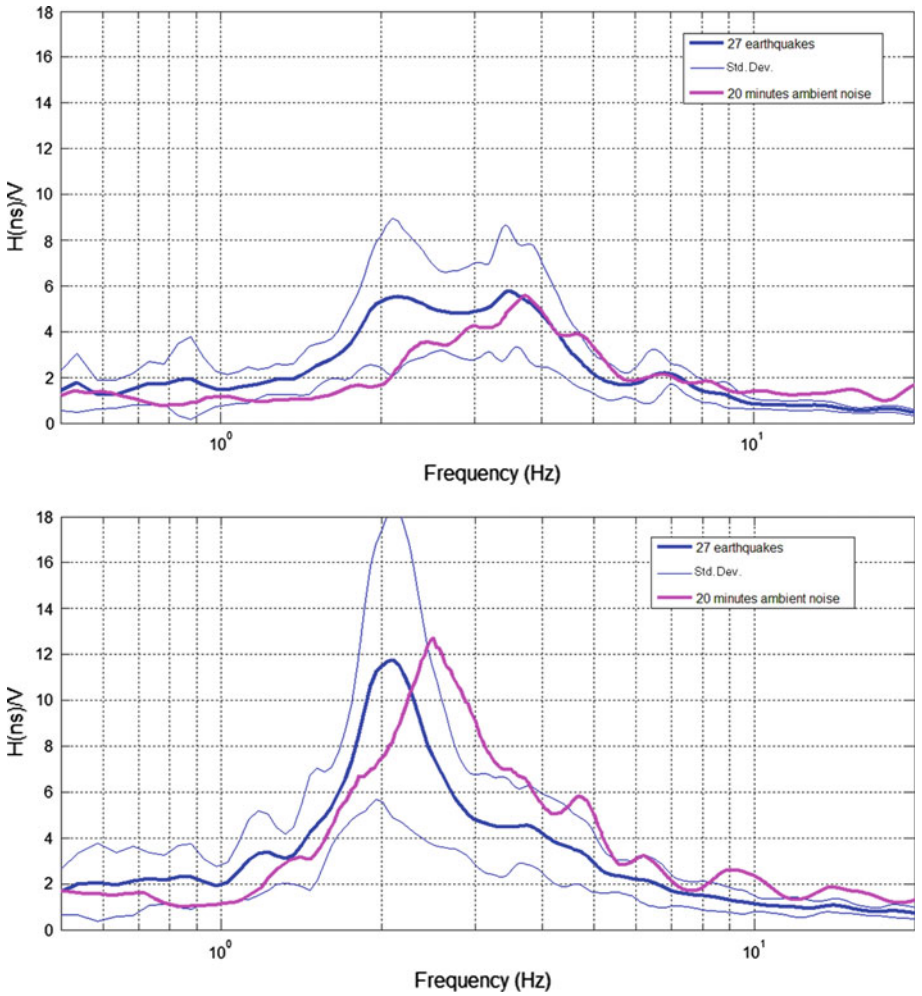

Fig. 11 HVSR curves for the two components (NS on the *top* and WE on the *bottom*) by 27 earthquakes and 20 min of ambient noise recordings

a clear resonance peak at about 2.6 Hz. This ambient noise HVSR has been validated by HVSR calculated on the 27 earthquakes of Table 1, according with the technique proposed by Lermo and Chàvez-Garcìa (1993) and Castro et al. (1997).

It is interesting to note the satisfactory agreement between the two HVSR curves not only in detection of frequency and amplitude of resonance peak but also in the shape. The H/V obtained from earthquakes shows a slight decrease in the frequency and amplitude of the main peak respect to the H/V from noise recordings probably due to a non-linear effect.

Moreover, even the ambient noise HVSR curves show a clear directional effect as highlighted by earthquake HVSRs. Figure 12 shows a strong directionality revealed with earthquakes and ambient noise HVSR at about 2 Hz. The slight difference in angle is due to the

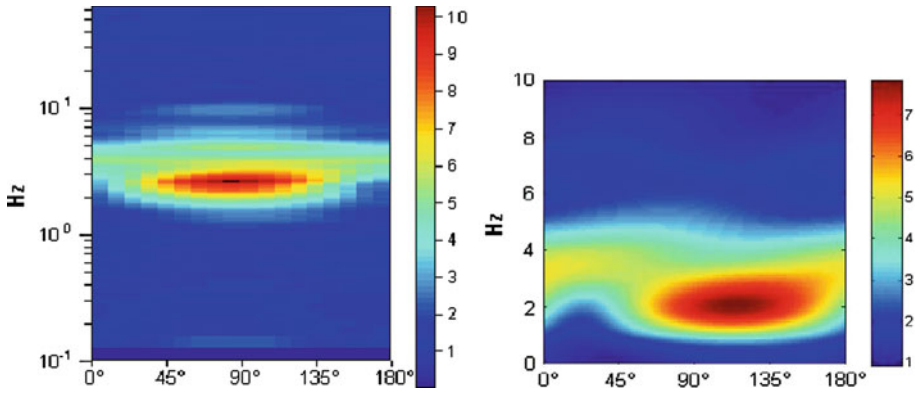

Fig. 12 Horizontal to vertical moving angle ratio by ambient noise recordings (*left*) and by 27 earthquakes (*right*)

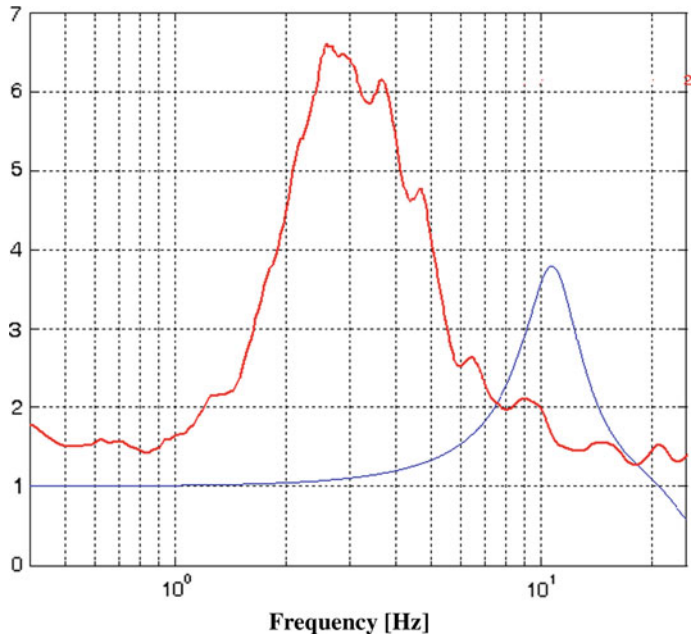

Fig. 13 Comparison between ambient noise HVSR (*red*) and 1-D model (*blue*)

fact that the accelerometer was pointed to true North, while the tromometer was aligned with the maximum slope direction.

This peculiar and strong directionality might suggest a 2D effect. In fact, a 1D model has been performed considering the values of the velocity taken from the down-hole and the stratigraphy of the geognostic borehole carried out close to the collapsed building (see Figs. 6, 8). The model curve highlights a resonance peak at a frequency much higher than the one estimated by earthquake and ambient noise HVSR (10 Hz vs. 2.5 Hz, Fig. 13).

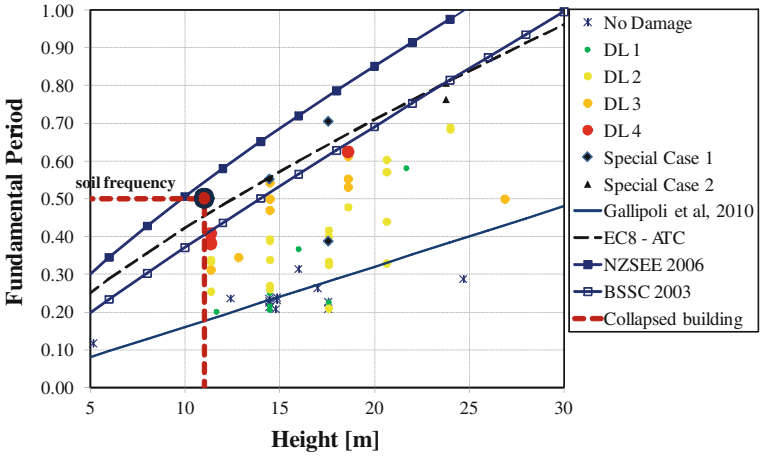

Fig. 14 Correlation among height–period–damage level (modified from Ditommaso et al. 2010)

6 Discussion and conclusions

The analyses of building type, material and design show that for the San Gregorio collapsed building probably the structural vulnerability was not the main determinant on the storey mechanism observed. In fact, even though the collapse was due to a storey mechanism the building (the farthest-from-epicentre collapsed building) did not have a soft story. On the contrary the study of the site effects returns a very high amplification of seismic motion along the same direction where the building was displaced of more than 70 cm. At the moment it is not possible to model the observed amplification: the 1-D profile returned from down–hole gives a fundamental frequency much higher than the observed one. The strong lateral variation visible in the ERT tomography suggests at least a 2-D effect but more data are required to study 3-D, out-of-plane geometry. A further consideration involves possible soil-building resonance. This phenomenon was considered for other structural damages that our research group observed on single instances (Mucciarelli et al. 2004; 2011). In this case we think that it is unlikely that resonance occurred. Of course it is impossible to measure the building fundamental period, even the post damage one; however, we can try to assess it from a statistical point of view. We know the average period-height relationship for undamaged RC buildings in southern Europe (Gallipoli et al. 2010) and for L'Aquila we have also an estimate of buildings period elongation as a function of damage (Ditommaso et al. 2010). Figure 14 shows that for a building 11 m tall the average elastic undamaged period is about 0.18 s while even for the highest degrees of damage no buildings was observed to reach a post yield period of 0.5 s, that is the soil observed period. We then think that for the collapsed building the main culprit is a peculiar site effect due to an unexpected thickness of fault cataclastic material just below the building, not visible from a surface survey, and whose genesis and deposition geometry over the bedrock should be further investigated.

Acknowledgments We acknowledge the financial support of MIUR-PRIN 2007 S.T.E.S.S.A. and by Microzonation project for L'Aquila—Department of Civil Defence. We thank the Task Force of GFZ, Potsdam, for the data of the accelerometric station.

References

ATC (1978) Tentative provisions for the development of seismic regulations for buildings, Report N. ATC3-06, Applied Technology Council, California

BSSC (2003) NEHRP Recommended provisions for seismic regulations for new buildings and other structures (FEMA 450), 2003 Edition, Building Seismic Safety Council, Washington DC

CEN (2005) Eurocode 8: Design provisions for earthquake of structures—part 1–4: strengthening and repair of buildings. European Prestandard ENV 1998-1-4. Comite European de Normalisation, Brussels

Caputo R, Piscitelli S, Oliveto A, Rizzo E, Lapenna V (2003) The use of electrical resistivity tomographies in active tectonic: examples from the Tyrnavos Basin, Greece. J Geodyn 36:19–35

Castro RR, Mucciarelli M, Pacor F, Petrungaro C (1997) S-Wave site-response estimates using horizontal-to-vertical spectral ratios. Bull Seism Soc Am 87:256–260

Chatelain J-L, Guillier B, Cara F, Duval A-M, Atakan K, Bard P-Y and the WP02 SESAME team (2008) Evaluation of the influence of experimental conditions on H/V results from ambient noise recordings. Bull Earthq Eng. doi:10.1007/s10518-007-9040-7

Compagnoni M, Pergalani F, Boncio P (2010) Microzonation study in the Paganica-San Gregorio area affected by the April 6, 2009. L'Aquila earthquake (central Italy) and implications for the reconstruction, Bull Earthq Eng. doi:10.1007/s10518-010-9226-2

Dahlin T (2001) The development of DC resistivity imaging techniques. Comput Geosci 27:1019–1029

Ditommaso R, Gallipoli MR, Mucciarelli M, Vona M (2010) Damage level versus fundamental frequencies of damaged RC buildings. The dynamic interaction of soil and structure. L'Aquila, 19 March 2010. pp 204. ISBN 978-88-548-3693-8. Aracne editrice, Ariccia (Roma) (in press)

Dolce M, Masi A, Ferrini M (2006) Estimation of the actual in-place concrete strength in assessing existing RC structures. The Second International fib Congress, June 5–8, 2006, Naples, Italy

Galli P, Bosi V, Piscitelli S, Giocoli A, Scionti V (2006) Late Holocene earthquakes in southern Apennines: paleoseismology of the Caggiano fault. Int J Earth Sci (Geol Rundsch) 95(5):855–870. doi:10.1007/s00531-005-0066-2

Galli P, Camassi R (eds) (2009) Rapporto sugli effetti del terremoto aquilano del 6 aprile 2009, Rapporto congiunto DPC-INGV, 12 pp. Web page: http://portale.ingv.it/real-time-monitoring/quest/aquilano-06-04-2009

Gallipoli MR, Mucciarelli M, Šket-Motnikar B, Zupančić P, Gosar A, Prevolnik S, Herak M, Stipčević J, Herak D, Milutinović Z, Olumćeva T (2010) Empirical estimates of dynamic parameters on a large set of European buildings. Bull Earthq Eng 8(3): 593–607. doi:10.1007/s10518-009-9133-6

Giano SI, Lapenna V, Piscitelli S, Schiattarella M (2000) Electrical imaging and self-potential surveys to study the geological setting of the Quaternary slope deposits in the Agri high valley (Southern Italy). Ann Geofis 43:409–419

Griffiths DH, Barker RD (1993) Two-dimensional resistivity imaging and modelling in areas of complex geology. J Appl Geophys 29:211–226

Herak M (2008) ModelHVSR—A Matlab tool to model horizontal-to-vertical spectral ratio of ambient noise. Comp Geosci doi:10.1016/j.cageo.2007.07.009

Lermo J, Chàvez-Garcìa FJ (1993) Site effect evaluation using spectral ratios with only one station. Bull Seism Soc Am 83:1574–1594

Loke MH, (2001) Tutorial: 2-D and 3-D electrical imaging surveys. In: Course notes for USGS workshop "2-D and 3-D inversion and modeling of surface and borehole resistivity data", Storrs, CT, 13–16 March 2001

Masi A, Vona M (2009) Estimation of the in-situ concrete strength: provisions of the European and Italian seismic codes and possible improvements. Convegno Finale del Progetto ReLUIS-DPC 2005–2008. Naples, 1–3 aprile 2009. Available at www.reluis.it

Masi A, Vona M (2010) Experimental and numerical evaluation of the fundamental period of undamaged and damaged rc buildings. Bull Earthq Eng. Special Issue Ambient Noise. 8(3):643–656. doi:10.1007/s10518-009-9136-3. ISSN: 1570-761X

Mucciarelli M, Masi A, Gallipoli MR, Harabaglia P, Vona M, Ponzo F, Dolce M (2004) Analysis of RC building dynamic response and soil-building resonance based on data recorded during a damaging earthquake. Bull Seismol Soc Am 94(5): 1943–1953. doi:10.1785/012003186

Mucciarelli M, Bianca M, Ditommaso R, Gallipoli MR, Masi A, Milkereit C, Parolai S, Picozzi M, Vona M (2011) Far field damage on RC buildings: the case study of Navelli during the L'Aquila (Italy) seismic sequence, 2009. Bull Earthq Eng. 9(1). doi:10.1007/s10518-010-9201-y. ISSN: 1570-761X

NZSEE (2006) Assessment and improvement of the structural performance of buildings in earthquakes, Recommendations of a NZSEE Study Group on Earthquake Risk Buildings

Parolai S, Galiana-Merino JJ (2006) Effect of transient seismic noise on estimates of H/V spectral ratios. Bull Seismol Soc Am 96:228–236
Sasaki Y (1992) Resolution of resistivity tomography inferred from numerical simulation. Geophys Prospect 54:453–464
Sharma PV (1997) Environmental and engineering geophysics. Cambridge University Press, Cambridge